PHYSICAL REVIEW D **84,** 033007 (2011)

Covariant model for the $\gamma N \to N(1535)$ transition at high momentum transfer

G. Ramalho[1] and M. T. Peña[1,2]

[1]*CFTP, Instituto Superior Técnico, Universidade Técnica de Lisboa, Av. Rovisco Pais, 1049-001 Lisboa, Portugal*
[2]*Dep. Física, Instituto Superior Técnico, Universidade Técnica de Lisboa, Av. Rovisco Pais, 1049-001 Lisboa, Portugal*

(Received 25 May 2011; published 9 August 2011; publisher error corrected 11 August 2011)

A relativistic constituent quark model is applied to the $\gamma N \to N(1535)$ transition. The $N(1535)$ wave function is determined by extending the covariant spectator quark model, previously developed for the nucleon, to the S_{11} resonance. The model allows us to calculate the valence quark contributions to the $\gamma N \to N(1535)$ transition form factors. Because of the nucleon and $N(1535)$ structure the model is valid only for $Q^2 > 2.3$ GeV^2. The results are compared with the experimental data for the electromagnetic form factors F_1^* and F_2^* and the helicity amplitudes $A_{1/2}$ and $S_{1/2}$, at high Q^2.

DOI: 10.1103/PhysRevD.84.033007 PACS numbers: 13.40.Gp, 12.39.Ki, 14.20.Gk

I. INTRODUCTION

The quark and gluon substructure of the hadrons is ruled by quantum chromodynamics (QCD), and it is reflected in the baryon sector by a set of bumps in the cross sections of different probing processes, taken as functions of the center of mass energy W. These bumps are identified as baryon resonances characterized by spin, isospin, orbital angular momentum, radial excitation and parity quantum numbers. The lowest energy bump, the $\Delta(1232)$ baryon, is clearly isolated from the background as a state of spin and isospin $3/2$ and positive parity. Heavier resonances are not so clearly isolated from the background. This happens in the so-called second resonance region, where the $P_{11}(1440)$, $D_{13}(1520)$, and $S_{11}(1535)$ resonances show up. Although in quark models these resonances can be described as three-quark systems confined by a potential like the harmonic-oscillator potential [1–5], some properties, like their decay width, can be better understood within a dynamical meson-baryon coupled-channel reaction model. Also, in constituent quark models the baryon spectrum is difficult to interpret since the negative parity partner of the nucleon, the S_{11} state ($J^P = \frac{1}{2}^-$) is lighter than the first radial excitation of the nucleon ($J^P = \frac{1}{2}^+$), the Roper (or P_{11} state) [3,6]. It was only recently that lattice QCD simulations with very small pion masses [6], reconstructed the natural order of the baryon spectrum (where the S_{11} state is heavier than the P_{11} state), suggesting a fundamental role of the quark-antiquark polarization, or meson cloud dressing, in the baryon systems, as a correction to the valence quark effects.

In this work, we will use the notation $N(1535)$ to represent the $S_{11}(1535)$ nucleon excitation (N), and we will focus on the electromagnetic structure of this resonance, in particular, on the calculation of the $\gamma N \to N(1535)$ transition form factors, within a covariant constituent quark model. Precise data for the $\gamma N \to N(1535)$ amplitudes is available at present [7–14]. Besides being one of the lightest nucleon resonances, the $N(1535)$ baryon is particularly interesting for several reasons: it is very well isolated in the spin $1/2$ and negative parity configuration; it decays strongly to the ηN channel (with a branching ratio $\approx 50\%$), allowing a very precise determination of the electromagnetic structure, and providing therefore an extra challenge for theoretical models. Also, because of the strong coupling with the πN channel (with a branching ratio $\approx 50\%$), the $N(1535)$ is crucial for the analysis of meson photoproduction from the nucleon [14]. Another interesting aspect of the $N(1535)$ is its vicinity to another S_{11} resonance with higher mass, the $S_{11}(1650)$ also called as $N(1650)$. The two resonances differ in their decay modes, and the differences in their structure is yet to be explored.

Several formalisms have been used to describe the $N(1535)$ system. They are based either on quark models or on effective meson-baryon interaction models. In the first case, there are nonrelativistic constituent quark models [4,5,15–22], relativistic quark models [18,23–25], quark models with explicit quark-antiquark contributions [26], and QCD sum rules [27]. Alternatively, in the second case, the $N(1535)$ is interpreted as a molecular-type state dynamically generated by the meson-nucleon interaction [28–37] with a particular dominance of the $K\Sigma$ quasibound state [28,29,32]. A particular class of effective meson-baryon interaction models are the dynamical coupled-channel reaction models [8,22,38–42], where the baryon bare core is parametrized phenomenologically and the meson dressing is included non perturbatively. Thus, $N(1535)$ does not only provide a crucial test for the methods just mentioned, but it is also a crucial resonant structure for the analysis of nucleon excitation reactions [7,8,14,42–49].

Within a constituent quark model picture, the nucleon excitation $N(1535)$ can be represented as a mixture of two different configurations. Since the S_{11} excitation has total angular momentum $J = 1/2$ and orbital angular $L = 1$ (P state excitation), its core spin may be either $S = 1/2$ or $S = 3/2$. Then, in the usual spectroscopic notation [3,32], the S_{11} channel of the nucleon excitation is a mixture of the $|N^2P_{1/2}\rangle$ and $|N^4P_{1/2}\rangle$ states, which have

spin $1/2$ and $3/2$ respectively. This mixture of the two core spin components is defined by a mixing angle θ_S determined by a color hyperfine interaction between the quarks, which may have distinct origins: one-gluon-exchange [3–5], one-pion-exchange [32] or Goldstone-boson-exchange [50]. In the classical Isgur-Karl model, it turns out that the spin core spin $1/2$ component dominates in the $N(1535)$, with a mixing angle given by $\cos\theta_S = 0.85$ [4,5].

In our work, we apply the covariant spectator quark model, which is based on the covariant spectator theory [51], to the $N(1535)$ system. The model describes the nucleon [52–55], the Roper [56,57], the $\Delta(1232)$, and the $\Delta(1600)$ [54,57–63] experimental form factors, as well as the lattice QCD simulations for the nucleon, the $\gamma N \to \Delta$ transition, and the baryon decuplet [54,60,64,65]. In our framework the baryons are represented as a quark-diquark system. The quark couples to the electromagnetic field by means of a constituent quark current which is parametrized by vector meson dominance, and the diquark is a spectator during the electromagnetic interaction, and therefore is taken on-mass-shell [52,59,62,64]. The model is phenomenological since it does not derive the structure of the baryon from a dynamical wave function equation. Instead, the baryon systems are described effectively in terms of their intrinsic properties (spin, flavor, angular orbital momentum and parity)—which dictate the form of their wave function—and the experimental value of their mass M_B. As in the previous applications of the model, in particular, to the Δ and the Roper resonances, we are focused on the role of the valence quarks for the electromagnetic transition. Because of this and also as a consequence of the kinematics (the difference of mass between the $N(1535)$ and the nucleon is 0.60 GeV), our model can only be applied to the high Q^2 region. As we will show, the domain of validity of our calculations can even be established more precisely and quantitatively, as the region $Q^2 > 2.3$ GeV^2. In this region, the meson cloud effects are expected to be small and valence quark degrees to dominate. We use two additional assumptions: i) the $N(1535)$ is represented exclusively by the spin $1/2$ core [no mixture with the $N(1650)$ excitation] ii) the diquark is pointlike. With these assumptions, and taking the momentum distribution of the diquark the same as for the nucleon, we relate the nucleon and the $N(1535)$ wave functions. These assumptions allow us to reduce the number of degrees of freedom to a minimum, since no additional parameters to the ones taken for the nucleon case are needed to describe the spin $3/2$ core contributions, or the diquark internal structure. Our results are then true predictions, with no new adjustable parameters. All parameters were fixed in the previous applications by the quark current and nucleon wave function, represented as S-wave system. Both assumptions can be tested in the future, once the structure of the nucleon is extended to the inclusion of P- and D-states, which demand in turn a spin $3/2$ core and/or diquark with internal P-state structure [66].

This work will be organized as follows: In Sec. II, we introduce the wave functions of the nucleon and the $N(1535)$ (details in Appendix A). In Sec. III, we derive the transition current for the $\gamma N \to N(1535)$ transition (with details presented in Appendix B). Explicit formulae for the form factors and helicity amplitudes come in Sec. IV. In Sec. V, we parametrize the momentum dependence of the wave functions. The results and discussion are presented in Sec. VI and the conclusions in Sec. VII.

II. SPECTATOR QUARK MODEL

When the momentum transfer exceeds the mass of the constituent quarks, the electromagnetic excitation requires necessarily a relativistic treatment. This is one of the reasons for us to use the framework provided by the covariant spectator quark model for baryons [52]. In this formalism, the baryons are phenomenologically described as constituent quark systems, and the covariant wave function has a form compatible with their symmetry properties (flavor, spin, orbital angular momentum and parity) and a totally antisymmetric color wave function [52,56,59,64].

A. Nucleon wave function

For the nucleon, the S-state approximation was made and the spin, flavor and spatial wave function and is represented by [52]

$$\Psi_N(P,k) = \frac{1}{\sqrt{2}}[\phi_I^0 u(P) - \phi_I^1 (\varepsilon_P^*)_\alpha U^\alpha(P)]\psi_N(P,k), \quad (1)$$

where the nucleon and diquark four momenta are P and k respectively, u is a Dirac spinor, ε_P the diquark polarization vector in the fixed-axis representation [53] and

$$U^\alpha(P) = \frac{1}{\sqrt{3}}\gamma_5\left(\gamma^\alpha - \frac{P^\alpha}{M}\right)u(P), \quad (2)$$

the spin $1/2$ vector spin state [direct product of states 1 (diquark) and $1/2$ (quark) for a total spin state of $1/2$]. M is the nucleon mass. The wave function (1) is written in terms of the states corresponding to a diquark composed by the quark-pair (12) and the quark 3. The isospin functions $\phi_I^{0,1}$ depend on the isospin projection $\pm 1/2$ and are shown in Table I. Note that the spin-0 (isospin-0) and the spin-1 (isospin-1) states are, respectively, antisymmetric and symmetric in the exchange of quarks 1 and 2.

TABLE I. Isospin states for the nucleon and S_{11} systems.

	ϕ_I^0	ϕ_I^1
p	$\frac{1}{\sqrt{2}}(ud - du)u$	$\frac{1}{\sqrt{6}}[(ud + du)u - 2uud]$
n	$\frac{1}{\sqrt{2}}(ud - du)d$	$\frac{1}{\sqrt{6}}[2ddu - (ud + du)d]$

B. $N(1535)$ wave function

To write down the $N(1535)$ wave function, we applied the $SU(3) \otimes O(3)$ constituent quark model representation, where the $N(1535)$ state is a member of the $[70, 1^-]$ supermultiplet (dimension 70, with $L^P = 1^-$), and part of the $^2 8$ subset (octet with $2S + 1 = 2$) [1,3–5,15–17]. We have also followed very closely the notation established in Refs. [3,14,67,68]. We use M_S to label the $N(1535)$ mass.

The $N(1535)$ is defined as the excitation of the nucleon to the state $I(J^P) = \frac{1}{2}(\frac{1}{2})^-$. This state has the same flavor content and the same spin $(1/2)$ of the nucleon, but has negative parity. The negative parity defines a spatial symmetry implied by the excitation of internal relative angular momentum $L = 1$, and requires the presence of P waves at least in one quark-pair. Consequently, the spin structure also changes relatively to the one of the nucleon, in order to accommodate a total symmetric form for the flavor-spin-momentum space wave function.

To represent the wave function in a basis of momentum states, one decomposes, as usual, the system into a pair of quarks [or diquark labeled (12)], and a spectator quark [labeled quark (3)], and one defines the momentum variables corresponding to those diquark and spectator quark subsystems (the so-called Jacobi momenta). If the individual quark momenta are k_i $(i = 1, 2, 3)$, the Jacobi momenta are $k_\rho = \frac{1}{\sqrt{2}}(k_1 - k_2)$, the relative momentum of the quarks in diquark (12), and $k_\lambda = \frac{1}{\sqrt{6}}(k_1 + k_2 - 2k_3)$, the diquark center of mass momentum with respect to quark (3). The center of mass momentum is $P = k_1 + k_2 + k_3$. The momentum states that define our basis to represent the wave function are the eigenvectors of the Jacobi momenta k_λ and k_ρ. They are called λ-type and ρ-type states, with mixed symmetry.[1] Following the traditional notation (see e.g. Ref. [18,20,38]), the labels ρ and λ are used more generally, i.e., for combinations and angular momentum projections of momentum states, and also for spin and isospin states, that are, respectively, antisymmetric and symmetric under the exchange of quarks (12).

The starting point for the construction of the flavor-spin-momentum-space wave function is to impose that it is symmetric under the exchange of any pair (the color part, which is omitted, makes it antisymmetric at the end, as required). The second step is to write the nonrelativistic limit of the wave function in terms of λ-type and ρ-type mixed-symmetric states, labeled X_ρ and X_λ, that couple orbital states $L = 1$ (in principle in both k_ρ and k_λ Jacobi momenta) with total three-quark spin $S = 1/2$ states, and to multiply them with the adequate flavor states that make the function symmetric. Next, we assume a pointlike diquark. In this approximation, effectively, one has $k_\rho \equiv 0$. With this suppression of the diquark internal P states, the orbital wave function is reduced to P-states in the momentum k_λ of the quark-diquark motion only. Additionally, the nonrelativistic wave function is calculated in the 3 body center of mass frame, where $\mathbf{k_1} + \mathbf{k_2} + \mathbf{k_3} = \mathbf{0}$, and the diquark three momentum becomes $\mathbf{k} = \mathbf{k_1} + \mathbf{k_2} = -\mathbf{k_3}$. Then, the spin-orbital part of the nonrelativistic wave function is, in our approximation, written as a function of $\mathbf{k}_\lambda = \sqrt{\frac{3}{2}}\mathbf{k}$ only.

Finally, one makes the relativistic generalization of the coupled spin-orbital states X_ρ and X_λ. The corresponding relativistic states, labeled respectively Φ_ρ and Φ_λ, include a γ_5 matrix, exhibiting the negative parity of the state explicitly. All the details concerning the full nonrelativistic wave function in the pointlike diquark limit, and its relativistic generalization, are presented in Appendix A. To conclude this section, we write in the pointlike diquark approximation, the final expression for the covariant structure of the spin-flavor-orbital wave function of the $N(1535)$. It depends on the baryon four-momentum P and on the diquark four-momentum k, and is given by

$$\Psi_{S11}(P, k) = \frac{1}{\sqrt{2}}[\phi_I^0 \Phi_\rho - \phi_I^1 \Phi_\lambda]\psi_{S11}(P, k), \quad (3)$$

where ϕ_I^0 and ϕ_I^1 are the flavor states, and

$$\begin{aligned}\Phi_\rho(\pm) &= -\gamma_5 N[(\varepsilon_0 \cdot \tilde{k})u_S(\pm) - \sqrt{2}(\varepsilon_\pm \cdot \tilde{k})u_S(\mp)] \\ \Phi_\lambda(\pm) &= +\gamma_5 N[(\varepsilon_0 \cdot \tilde{k})\varepsilon_\alpha^* U_S^\alpha(\pm) - \sqrt{2}(\varepsilon_\pm \cdot \tilde{k})\varepsilon_\alpha^* U_S^\alpha(\mp)].\end{aligned} \quad (4)$$

In the last equations $\tilde{k} = k - \frac{P \cdot k}{M_S^2} P$ and $N = 1/\sqrt{-\tilde{k}^2}$, the four-momentum $\tilde{k}$ can be interpreted as the diquark three momentum in the $N(1535)$ rest frame [where $\tilde{k} = (0, \mathbf{k})$ and $\tilde{k}^2 = -\mathbf{k}^2$]. The spinors u_S and U_S^α have the same meaning as u and U^α, defined for the nucleon before [52,58,59], as in Eq. (2), but are here associated with the $N(1535)$ baryon.

The scalar wave function $\psi_{S11}(P, k)$ will be discussed later (see Sec. V). Here, it suffices to say that this function carries all the information on the momentum distribution of the quark-diquark relative motion, it is purely phenomenological and normalized to one.

We make two more notes about Eq. (3): The wave function in our model does not contain the contribution of three-quark states with total spin $S = 3/2$, included in other works [4,18,32]. Additionally, the minus sign for the λ-type spin-orbital in the wave function is needed to ensure orthogonality between the $N(1535)$ and the nucleon wave functions in the nonrelativistic limit [32].

[1]The Jacobi momentum k_ρ is antisymmetric for the exchange of quarks 1 and 2, while the Jacobi momentum k_λ is symmetric for the same exchange. The Jacobi momenta k_ρ and k_λ eigenvector basis states are, therefore, antisymmetric and symmetric, respectively, under that exchange. For another particle exchange $i \rightarrow j$, with $(ij) \neq (12)$, those states are, however, states of mixed symmetry.

III. TRANSITION CURRENT

We can write the transition current in relativistic impulse approximation [52,64] as

$$J^\mu = 3\sum_\Lambda \int_k \bar{\Psi}_{S11}(P_+, k) j_I^\mu \Psi_N(P_-, k), \tag{5}$$

where $\Lambda = \{s, \lambda_D\}$ (scalar diquark s and vector diquark polarization $\lambda_D = 0, \pm 1$) and $\int_k \equiv \int \frac{d^3k}{(2\pi)^2 2E_D}$ is the covariant integration element in the diquark on-mass-shell momentum k (mass m_D and energy E_D). The factor 3 accounts for the contributions of all possible diquark pairs, since, due to the symmetry of the wave function, pairs (13) and (23) give the same contribution as pair (12). [The magnitude of the electron charge e was not included in the current for simplicity]. In the previous equation, j_I^μ is the quark current

$$j_I^\mu = j_1\left(\gamma^\mu - \frac{\not{q} q^\mu}{q^2}\right) + j_2 \frac{i\sigma^{\mu\nu} q_\nu}{2M}. \tag{6}$$

To obtain the $\gamma N \to N(1535)$ transition current, we take the wave functions (1) and (3). To work the spin algebra, one uses $j_i \to (\phi_I^0)^\dagger j_i \phi_I^0$ and $j_{(i+2)} = (\phi_I^1)^\dagger j_i \phi_I^1$, obtaining

$$j_i = \frac{1}{6} f_{i+} + \frac{1}{2} f_{1-}\tau_3 \tag{7}$$

$$j_{(i+2)} = \frac{1}{6} f_{i+} - \frac{1}{6} f_{i-}\tau_3. \tag{8}$$

The coefficients $j_{1,2}$ and $j_{3,4}$ follow the definitions in Ref. [52]. Note that the result is a sum over the flavor of the antisymmetric (j_1 and j_2) and symmetric components (j_3 and j_4) as done in Refs. [55,64] for the SU(3) case. For convenience, one introduces also the notation

$$\hat{\gamma}^\mu = \gamma^\mu - \frac{\not{q} q^\mu}{q^2}. \tag{9}$$

Using the definitions above, one can write

$$\sum_\Lambda \bar{\Psi}_{S11} j_I^\mu \Psi_N = \frac{\mathcal{A}}{2}\left\{ j_1 \bar{\Phi}_\rho \hat{\gamma}^\mu \phi_S^0 + j_2 \bar{\Phi}_\rho \frac{i\sigma^{\mu\nu} q_\nu}{2M} \phi_S^0 \right\} - \frac{\mathcal{A}}{2}\left\{ j_3 \bar{\Phi}_\lambda \hat{\gamma}^\mu \phi_S^1 + j_4 \bar{\Phi}_\lambda \frac{i\sigma^{\mu\nu} q_\nu}{2M} \phi_S^1 \right\}, \tag{10}$$

where $\mathcal{A} = \psi_{S11}\psi_N$. For the vector diquark contributions (terms in ϕ_S^1), the sum in the diquark polarization λ_D is implicit. The isovector components include a sum in the diquark polarizations λ_D vectors associated with the $N(1535)$, $\varepsilon_{P_+}^\alpha(\lambda_D)$, and the nucleon, $\varepsilon_{P_-}^{\beta *}(\lambda_D)$. Those polarization vectors are functions of the $N(1535)$ mass (M_S) and the nucleon (M) mass, respectively, (see details in Ref. [53] where this basis of states is explained and built). By adding the diquark polarizations, one has [53,58]

$$\Delta^{\alpha\beta} \equiv \sum_{\lambda_D} \varepsilon_{P_+}^\alpha(\lambda_D)\varepsilon_{P_-}^{\beta *}(\lambda_D) = -\left(g^{\alpha\beta} - \frac{P_-^\alpha P_-^\beta}{P_+ \cdot P_-}\right) - a\left(P_- - \frac{P_+ \cdot P_-}{M_S^2} P_+\right)^\alpha \times \left(P_+ - \frac{P_+ \cdot P_-}{M^2} P_-\right)^\beta, \tag{11}$$

where

$$a = \frac{M_S M}{P_+ \cdot P_-(M_S M + P_+ \cdot P_-)}. \tag{12}$$

The decomposition (10) reduces the determination of the current (5) to the calculation of a few current elements. The details are presented in Appendix B. The final result is

$$J^\mu = \frac{1}{2}(3j_1 + j_3)\mathcal{I}_0 \bar{u}_S \hat{\gamma}^\mu \gamma_5 u - \frac{1}{2}(3j_2 - j_4)\mathcal{I}_0 \bar{u}_S \frac{i\sigma^{\mu\nu} q_\nu}{2M}\gamma_5 u, \tag{13}$$

where

$$\mathcal{I}_0(Q^2) = \int_k N(\varepsilon_0 \cdot \tilde{k})\psi_{S11}\psi_N. \tag{14}$$

The integral $\mathcal{I}_0$ is covariant and includes the dependence of the form factors on the initial and final state scalar wave functions. We call $\mathcal{I}_0$ the overlap integral.

IV. FORM FACTORS AND HELICITY AMPLITUDES

The transition current can be written (suppressing the charge factor e) as [20,27]:

$$J^\mu = \bar{u}_S\left[\left(\gamma^\mu - \frac{\not{q} q^\mu}{q^2}\right)F_1^* + \frac{i\sigma^{\mu\nu} q_\nu}{M_S + M} F_2^*\right]\gamma_5 u, \tag{15}$$

where F_i^* defines the transition form factors. One should note that there are alternative but equivalent conventions for the two form factors [7,24,27].

From the Eqs. (13) and (15), we conclude that

$$F_1^*(Q^2) = \frac{1}{2}(3j_1 + j_3)\mathcal{I}_0 \tag{16}$$

$$F_2^*(Q^2) = -\frac{1}{2}(3j_2 - j_4)\frac{M_S + M}{2M}\mathcal{I}_0. \tag{17}$$

The experimental data is usually presented in terms of the helicity amplitudes in the final state (excited resonance) rest frame. The helicity amplitudes are defined from the projection of the current on the photon polarization states, ϵ_λ^μ and nucleon and resonance spin projections (in the resonance frame). For a resonance N^* with spin $1/2$, there are two independent amplitudes:

$$A_{1/2}(Q^2) = \mathcal{K}\left\langle N^*, +\frac{1}{2}\middle|\, \varepsilon_+ \cdot J \,\middle| N, -\frac{1}{2}\right\rangle, \tag{18}$$

$$S_{1/2}(Q^2) = \mathcal{K}\left\langle N^*, +\frac{1}{2}\left|\, \varepsilon_0 \cdot J \,\right| N, +\frac{1}{2}\right\rangle \frac{|\mathbf{q}|}{Q}. \quad (19)$$

Considering $N^* = N(1535)$, the multiplicative constant is

$$\mathcal{K} = \sqrt{\frac{2\pi\alpha}{K}}, \quad (20)$$

with $e = \sqrt{4\pi\alpha}$ is the magnitude of the electron charge with $\alpha \simeq 1/137$, and $K = \frac{M_S^2 - M^2}{2M_S}$. The variable $|\mathbf{q}|$ is the photon three momentum in the excitation, in the $N(1535)$ rest frame,

$$|\mathbf{q}| = \frac{\sqrt{Q_+^2 Q_-^2}}{2M_S}, \quad (21)$$

where $Q_\pm^2 = (M_S \pm M)^2 + Q^2$, with $Q^2 = -q^2$.

The helicity amplitudes can be represented in terms of the form factors [20]:

$$A_{1/2} = -2b\left[F_1^* + \frac{M_S - M}{M_S + M} F_2^*\right] \quad (22)$$

$$S_{1/2} = \sqrt{2} b (M_S + M) \frac{|\mathbf{q}|}{Q^2}\left[\frac{M_S - M}{M_S + M} F_1^* - \tau F_2^*\right], \quad (23)$$

with $\tau = \frac{Q^2}{(M_S + M)^2}$ and

$$b = e\sqrt{\frac{Q_+^2}{8M(M_S^2 - M^2)}}. \quad (24)$$

From Eqs. (16) and (17) one can make predictions for the form factors and compare the obtained results with the experimental data.

V. SCALAR WAVE FUNCTIONS

Our model is now completely defined, for the baryons and for the current, except for the scalar function ψ_{S11}, which is part of the wave function.

In the spectator quark model, the scalar wave functions depend on $(P - k)^2$ only, as the baryon and diquark are taken on-mass-shell. That dependence can be rewritten in terms of the adimensional variable

$$\chi_B = \frac{(M_B - m_D)^2 - (P - k)^2}{M_B m_D}, \quad (25)$$

where M_B is the baryon mass [nucleon or $N(1535)$] and m_D the diquark mass.

Within the S-wave approach, the scalar function in the nucleon wave function is given by [52]:

$$\psi_N(P, k) = \frac{N_0}{m_D(\beta_1 + \chi_N)(\beta_2 + \chi_N)}, \quad (26)$$

where N_0 is the normalization constant and β_i are adimensional parameters which measure the momentum scale of the quark-diquark interaction. As $\beta_2 > \beta_1$, β_2 defines the scale for the short distance range and β_1 the long distance range.

As the $N(1535)$ corresponds to a spin $1/2$ quark core with the same content of the nucleon, it is reasonable to consider a form for the scalar wave function similar to the one taken for the nucleon

$$\psi_{S11}(P, k) = \frac{N_1}{m_D(\beta_3 + \chi_{S11})(\beta_2 + \chi_{S11})}, \quad (27)$$

where N_1 is the normalization constant and β_3 a new range parameter. To start with, the same parameter β_2 ($\beta_2 > \beta_3$) can be used for the two cases, the $N(1535)$ and the nucleon, if one assumes that the two baryons differ only in the structure at large distances. Moreover, on the other hand, and inspired by the relativistic quark models with an harmonic-oscillator confinement [18,20], we consider that the nucleon and the $N(1535)$ may as well have the same momentum distributions at large distances—as expected for excitations of the same state—and we will thus also take $\beta_3 = \beta_1$. Then, the nucleon and the $N(1535)$ are described by the same scalar wave functions in their rest frame. We may say that this assumption is justified since in the chiral limit the nucleon and the $N(1535)$ will have the same mass and become two different parity states of the same particle. The difference between the momentum distributions in the nucleon and the $N(1535)$ come from the difference in the orbital angular momentum in their total wave functions. In the nonrelativistic limit, this angular dependence corresponds to $Y_{00}(\hat{k})$, a constant, for the nucleon, and $Y_{1m}(\hat{k})$, the P-state, for the $N(1535)$.

An alternative parametrization for the scalar wave functions would be to force the fit of β_3 to the data and to introduce a new parameter in our model. Since we will see that our parameter-free description was surprisingly successful, we did not face a good reason to assume different scalar functions for the nucleon and the $N(1535)$, and our results can be considered true predictions, once the nucleon is correctly described.

Overlap integral

The transition form factors depend on the orbital wave functions through their overlap integral $\mathcal{I}_0$, defined by Eq. (14). Terms that include integrations in k_x or k_y vanish because of the symmetries of the scalar wave function (as function of χ_B), as shown in Appendix B, and the integral $\mathcal{I}_0$ carries the signature of the angular momentum dependence of the nucleon and $N(1535)$ wave functions.

The overlap integral is covariant and it can be evaluated in any frame. One of the simplest calculations is the one that proceeds in the $N(1535)$ (final state) rest frame, (see Appendix C), where

$$\mathcal{I}_0(Q^2) = \int_k \frac{k_z}{|\mathbf{k}|} \psi_{S11}(P_+ \cdot k)\psi_{N\cdot}(P_- \cdot k). \quad (28)$$

In the $N(1535)$ rest frame, all the angular dependence of the wave functions is contained in ψ_N, given by Eq. (26). This dependence is expressed by

$$P_- \cdot k = EE_D + |\mathbf{q}|k_z, \tag{29}$$

where $|\mathbf{q}|$ is the photon three momentum in the $N(1535)$ rest frame, as defined in Eq. (21), E is the nucleon energy, and E_D the diquark energy. The numerical value of $\mathcal{I}_0(0)$ depends, therefore, on the existing symmetries in the variable k_z. The properties of the overlap integral $\mathcal{I}_0(Q^2)$ are discussed in Appendix C. In particular, for small $|\mathbf{q}|$, one has

$$\mathcal{I}_0(Q^2) \propto |\mathbf{q}|. \tag{30}$$

This result has important consequences and allows us to define the domain of validity of our model.

In what follows, we will label $|\mathbf{q}|$ in the $Q^2 = 0$ limit by $|\mathbf{q}|_0$. As the photon energy ω equals $|\mathbf{q}|_0$ at $Q^2 = 0$, one has then $|\mathbf{q}|_0 = \frac{M_S^2 - M^2}{2M_S}$, and according to Eq. (30), $\mathcal{I}_0(0) = 0$, if $M_S = M$. The relation $\mathcal{I}_0(0) = 0$ is then equivalent to the orthogonality condition between the $N(1535)$ and the nucleon wave functions. However, if $M_S \neq M$, the integral $\mathcal{I}_0(0)$ will be proportional to $|\mathbf{q}|_0 = \frac{M_S^2 - M^2}{2M_S}$. Consequently, $\mathcal{I}_0(0) \neq 0$, and the $N(1535)$ and the nucleon wave functions are not exactly orthogonal. This result has a dramatic implication since the nucleon and the $N(1535)$ should in fact be orthogonal. This is an artifact of the construction of the wave function from its nonrelativistic behavior, and of having imposed to it a covariant form with multiplicative scalar functions that were not derived from an ab-initio calculation. A simple picture of what happens is that the nucleon orbital (S-state) wave function (defined unambiguously only in the rest frame of the nucleon) is distorted by the boost to the rest frame of the $N(1535)$, and therefore is not orthogonal to the $N(1535)$ orbital (P-state) wave function. This implies that the overlap integral $\mathcal{I}_0(0)$ does not vanish. Still, if the masses of the initial and final state are equal, $Q^2 = 0$ implies $|\mathbf{q}|_0 = 0$, as mentioned, and there is no problem since there is no boost.

The fact that the integral (28) is not zero for $Q^2 = 0$ is therefore a limitation of our model when the initial final and initial states have different masses. However, the relation (30) can be used to establish the range of application of the model. The non orthogonality between the model wave functions of the initial and final state decreases as M_S approaches M. If the mass difference is negligible there is orthogonality to a certain extent. Then, $|\mathbf{q}|_0 = \frac{M_S^2 - M^2}{2M_S}$ is a parameter that measures the quality of our model approximations to the wave function. As $|\mathbf{q}|_0$ corresponds to the photon energy at $Q^2 = 0$ (at the photon point the energy equals the three momentum), it defines the natural momentum scale of the reaction. In the regime $Q^2 \gg |\mathbf{q}|_0^2$, one has $\mathcal{I}_0(0) \approx 0$, meaning that the nucleon and the $N(1535)$ states are *almost* orthogonal. As for the physical case $|\mathbf{q}|_0 \simeq 0.48$ GeV, $\mathcal{I}_0(0) \simeq 0$ for $Q^2 \gg 0.23$ GeV^2, and therefore, one can say that $Q^2 > 2.3$ GeV^2 establishes the threshold for the application of our model.

Summarizing, the present model has limitations in its applications at low Q^2, in particular, near $Q^2 = 0$, but can be used in the high Q^2 regime, for $Q^2 > 2$ GeV^2.

VI. RESULTS

With the model for the baryons and for the current depicted in the previous sections, we have calculates the $\gamma N \to N(1535)$ transition form factors given by Eqs. (16) and (17) and the helicity amplitudes given by Eqs. (22) and (23). No parameters of our model were adjusted to these observables.

We calculated only the positive isospin case ($I_z = +1/2$), corresponding to the excitation reaction from the proton, where the data at finite Q^2 for the helicity amplitudes is available [7–13]. We did not consider the neutron case ($I_z = -1/2$), since there is data only for $Q^2 = 0$, and our model is valid only for $Q^2 > 2.3$ GeV^2. The data from DESY [10] and from Jefferson Lab [9,11–13] are restricted only to the $A_{1/2}$ amplitude, assuming that the amplitude $S_{1/2}$ was negligible. That assumption was contradicted by the recent CLAS [7] and MAID [8] analysis. In the following, we use Ref. [7,8] where $A_{1/2}$ and $S_{1/2}$ were determined simultaneously. We will also compare our results with the Dalton *et al.* data [9], for $A_{1/2}$ at high Q^2 ($Q^2 > 5.4$ GeV^2), which is determined under the assumption that $S_{1/2} = 0$ [for large Q^2 the approximation $S_{1/2} = 0$ is better justified due to the falloff of $S_{1/2}$ at high Q^2].

A. Transition form factors

The results for the $\gamma N \to N(1535)$ form factors are shown in Fig. 1. The data for F_1^* and F_2^* was obtained by inverting the relations (22) and (23). In the figure, we represent also the CLAS data from Ref. [7] and the MAID analysis of Ref. [8], as well as the results from [9] (where $S_{1/2} = 0$). One can see that our model describes well the F_1^* data for for $Q^2 > 1.5$ GeV^2, in particular, that the model works in its regime of application $Q^2 > 2.3$ GeV^2. As for F_2^*, our model fails completely when compared with the experimental data. We predict positive values for F_2^*, contrarily to the data. Also, the magnitude differs strikingly from the data: the CLAS data is very close to zero for $Q^2 > 2$ GeV^2, in the region where our model gives a strong positive contribution. This disagreement can be interpreted in two ways. One possibility is that our model is limited because the internal diquark P-states were neglected in our model, and we will have to confirm their effects in a future work. Another possible interpretation is that, for F_2^* the valence quark effects, the only ones considered in our model are strongly canceled by the effect of the meson cloud polarization, not included in our model.

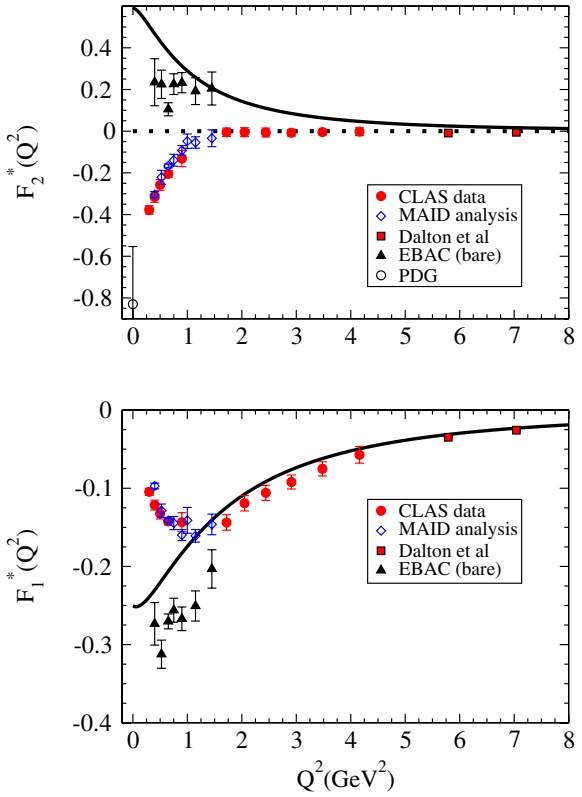

FIG. 1 (color online). $\gamma p \to N(1535)$ transition form factors. CLAS data from [7], MAID data from [8]. The EBAC results [40] corresponds to the transition when the meson cloud contribution is suppressed. The solid line is the prediction of the model. The data for $A_{1/2}(0)$ is given by Particle Data Group [73].

If this last interpretation is correct, one has to conclude that meson cloud effects are very significant, even in the region $Q^2 > 2$ GeV^2. This finding is at odds with what was observed till now in similar systems, like the nucleon [52] and the Roper [56]. Nevertheless, the $\gamma N \to \Delta$ quadrupole form factors reveal a strong contribution of the pion cloud in the region 2–6 GeV^2 [59,60].

To test the last interpretation, we compared our valence quark model predictions with the calculations from a different framework, the EBAC dynamical coupled-channel model based in Sato-Lee model [39]. In the EBAC analysis [40], the effects of the meson cloud dressing are subtracted, and the pure quark core contributions calculated from the model. The EBAC data can then be directly compared with our results, as shown also in Fig. 1 (upper triangles). As for F_1^*, the EBAC results overestimates (in absolute value) the experimental data (CLAS and MAID) but seems to approach the data for $Q^2 \approx 2$ GeV^2. As for F_2^*, the EBAC results are surprisingly consistent with our own predictions, both in sign and magnitude for $Q^2 \approx 1.5$ GeV^2, near the threshold where our model starts to be applicable, $Q^2 > 2.3$ GeV^2. Future EBAC determination of the quark core contributions, already planed for higher Q^2 [69], will be very important to test our predictions and interpretations. An independent confirmation of the large contribution of the valence quarks for F_2^* may also come from lattice QCD at high Q^2. We note that our covariant spectator quark model was already successful in the description of lattice QCD simulations for the nucleon, Roper [52,56,57] and Δ systems [54,60].

To summarize, our results for the form factor F_1^* are consistent with the data for $Q^2 > 2$ GeV^2, in the domain of validity of our model. As for F_2^*, our model supports the idea that meson cloud contributions are comparable with the valence quark contributions, which is also validated by the EBAC studies of the $N(1535)$ system [40].

B. Helicity amplitudes

Using our results for the form factors, we have also calculated the helicity amplitudes in the $N(1535)$ rest frame, corresponding to the transformations (22) and (23). Some comments are necessary before showing the results. The first note is that our quark model should be compared with the data only in the region $Q^2 > 2.3$ GeV^2. A second important note is that in our model $F_1^*(0) \neq 0$ because of the violation of the orthogonality condition between the nucleon and the $N(1535)$ wave functions. Therefore the amplitude $S_{1/2}$ in our model is singular for $Q^2 = 0$, in opposition to the finite result expected from the data. This effect was already reported in the relativistic quark model of Ref. [23], where the quark current was modified to restore gauge-invariance. With those limitations in mind, we represent in Fig. 2 the amplitudes corresponding to the form factors in Fig. 1, by the solid line. The dramatic deviation from the data is not surprising, since our model disagrees already with the F_2^* data. The disagreement is evident for $A_{1/2}$ where our large F_2^* contribution spoils a excellent result that would be obtained if the F_2^* could be neglected. The results obtained in that scenario $(F_2^*(Q^2) \equiv 0)$ are represented by the dashed line. In that case the agreement of our model with the data is excellent for $Q^2 > 2$ GeV^2 for both amplitudes. It is moreover interesting to note that the model (solid line) agrees well with the EBAC results for $S_{1/2}$. That comes from the F_1^* suppression in the $S_{1/2}$ amplitude by the factor $\frac{M_S - M}{M_S + M}$ [see Eq. (23)].

We conclude that the helicity amplitudes are not the best representation to test our model, since those amplitudes amplify the limitations of our model, like $F_1^*(0) \neq 0$ or the large magnitude of F_2^*. Combining our results for F_1^* with the assumption that F_2^* is negligible for $Q^2 > 2$ GeV^2, as a consequence of the meson cloud effect, which is substantiated by the data and the EBAC results, one can achieve a very good description of the helicity amplitudes data.

C. Comparison with the literature

The study of the $\gamma N \to N(1535)$ electromagnetic structure was in the past based almost only on the representation

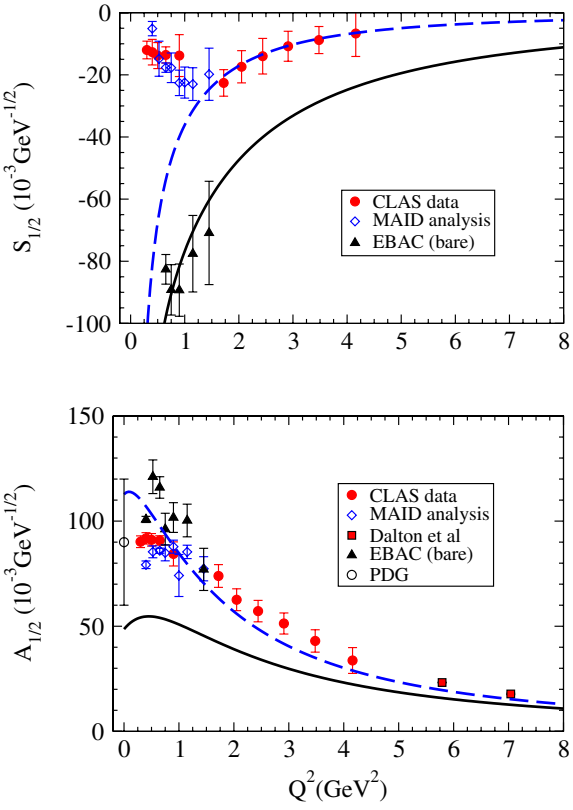

FIG. 2 (color online). $\gamma p \to N(1535)$ helicity amplitudes. CLAS data from [7], MAID data from [8]. The EBAC results [7] corresponds to the transition when the meson cloud contribution is suppressed. Particle data group data from Ref. [73]. The solid line is the prediction of the model. The dashed line is the result under the assumption that $F_2^* \equiv 0$ (as supported by the data).

of the helicity amplitudes [in the $N(1535)$ rest frame]. Then, the comparison with other works has to be done in this representation. From the previous section, we know that the data corresponds to positive values for $A_{1/2}$ and negative values for $S_{1/2}$.

We will start by discussing the constituent quark models. Different quark model predictions, including nonrelativistic [15,16,19–21] and relativistic [18,23–25] formulations, agree qualitatively with the data for $A_{1/2}$. In particular, in Ref. [18], calculations based on the light-front formalism give an excellent description of the $A_{1/2}$ data for $Q^2 > 2$ GeV^2 [7]. Also QCD sum rules [27] are consistent with the $A_{1/2}$ data for $Q^2 > 1$ GeV^2.

In a nonrelativistic model with harmonic-oscillator confinement potential, the relative sign between $A_{1/2}(0)$ and $S_{1/2}(0)$ is positive, and determined by the relative sign between the πNN and the $\pi NN(1535)$ coupling constants [20]. For nonrelativistic models, we should expect then positive values for $S_{1/2}$ at low Q^2. This feature is also shared by light-front and relativistic quark models [7,15,18,23,24], although sometimes negative results are obtained for $Q^2 > 2$ GeV^2 [7,18,24]. Still, in general one has the same sign for $A_{1/2}(0)$ and $S_{1/2}(0)$. Exceptions to this feature are obtained by the QCD sum rules [27] and our model. QCD sum rules predict the sign but underestimate in absolute value the result for $S_{1/2}$.

It has also been suggested that the state $N(1535)$ may have a strong contribution from quark-antiquark states, or even been dynamically generated by the meson-baryon interaction. An and Zou [26] considered a quark model with explicit quark-antiquark dressing, and concluded that those effects can be of the order of 20% for low Q^2. Overall, the signs and magnitudes are consistent with the data. In Ref. [22], the meson cloud dressing is calculated within the cloudy bag model. In that case the quark core is dominant at low Q^2 and is consistent with the data for $A_{1/2}$ (with $\approx 25\%$ of meson cloud), although the $S_{1/2}$ data is overestimated. For $Q^2 > 1.5$, the model predictions are suppressed compared with the data indicating that short range behavior is not well simulated by the bag model [22].

The helicity amplitudes were also determined using a chiral unitary approach [33,34]. The authors conclude that the $N(1535)$ seems to be largely dynamically generated from the interaction of mesons and baryons but also that a genuine quark component is necessary particularly at high Q^2 [34]. Qualitatively, the meson dressing explains roughly 50–60% of the $A_{1/2}$ amplitude. Also, the calculations of the EBAC group sugest the importance of the meson dressing at low Q^2, although there is a dominance of the quark core [40].

One may conclude that, in general, from quark models and hadronic models with meson dressing, the meson cloud can be important, but genuine valence quark contributions are equally necessary to explain the data.

D. Large Q^2 regime

The study of the asymptotic dependence of the $\gamma N \to N(1535)$ transition form factors attracts some attention, because pQCD predicts a very slow falloff for $A_{1/2}$ [70] and also because precise experimental data have been extracted at high Q^2, in particular, for $Q^2 \approx 4$ GeV^2 [11] and $Q^2 \simeq 5.7$, and 7.3 GeV^2 [9]. The estimate from pQCD [70] for large Q^2 is

$$Q^3 A_{1/2}(Q^2) = e\sqrt{\frac{M}{M_S^2 - M^2}}\beta, \tag{31}$$

where $\beta = 0.58$ GeV^3, in the more optimistic estimate (upper limit) [70]. As for the form factors, one expects $F_1^* \sim \frac{1}{Q^4}$ and $F_2^* \sim \frac{1}{Q^6}$, apart logQ^2 corrections. Then, for large Q^2, one has $|F_1^*| \gg |F_2^*|$, and, according to Eq. (22),

$$Q^4 F_1^*(Q^2) = -\sqrt{\frac{2M^2Q^2}{(M_S + M)^2 + Q^2}}\beta. \tag{32}$$

The asymptotic results from Eqs. (31) and (32) are presented in Fig. 3 for both F_1^* and $A_{1/2}$. In the last case, we

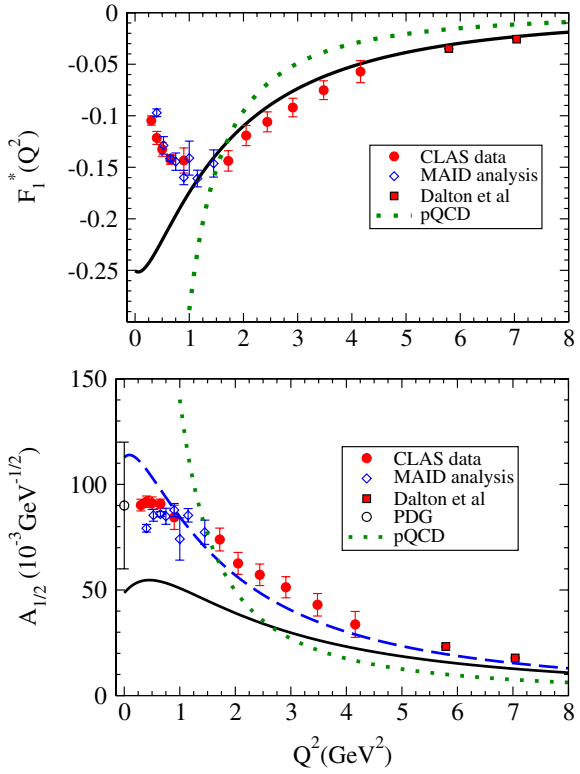

FIG. 3 (color online). $\gamma p \to N(1535)$ transition. Comparing $A_{1/2}$ amplitude and F_1^* with the asymptotic expressions. Same meaning of previous figures. The pQCD result is from Ref. [70].

show the result obtained by making $F_2^* = 0$, as discussed earlier. In the figure it is clear that the pQCD estimation underestimates the data and our model for high Q^2.

The asymptotic behavior of the form factors can be better understood scaling the functions by a convenient power of Q^2 to check if the results converge to a constant, apart the logarithm corrections. In this case, we should take the functions $Q^3 A_{1/2}$ and $Q^4 F_1^*$. The results for F_1^* are presented in Fig. 4. The representation of $A_{1/2}$ would be

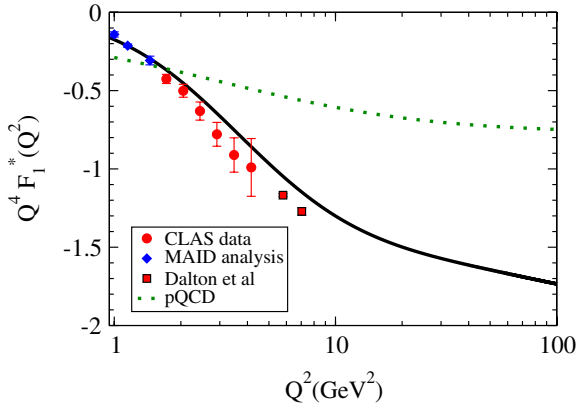

FIG. 4 (color online). $Q^4 F_1^*(Q^2)$ for high Q^2 compared with the data. The model (solid line) can be represented for high Q^2 as $Q^4 F_1^*(Q^2) \simeq -0.144 \log\frac{Q^2}{\Lambda^2}$ with $\Lambda^2 = 0.4982$ GeV^2.

equivalent. In the figure, it is clear that pQCD estimation fails the description of the data by a factor larger than 2. The same was reported in Ref. [9] for $A_{1/2}$. The pQCD prediction differs then from the spectator quark model. At $Q^2 = 100$ GeV^2 the ratio is 2.3. Also, in the figure it is clear a non constant slope for both pQCD and the spectator quark model results in the region shown, indicating corrections for the $1/Q^4$ behavior. In the pQCD case, the slope is a consequence of the Q^2-dependent factor of the r.h.s. of Eq. (32), which became a constant only for $Q^2 \gg (M_S + M)^2 = 6.1$ GeV^2 [see the slow variation of the dotted line in Fig. 4]. As for the spectator quark model, the logarithm dependence at larger Q^2, comes from the parametrization of the nucleon wave functions by Eq. (26), as product of two monopole factors in the variable $(P - k)^2$. That choice was considered in the applications to the nucleon electromagnetic structure [52] in order to reproduce the expected pQCD behavior for the nucleon form factors (Dirac $F_1 \sim \frac{1}{Q^4}$ and Pauli $F_1 \sim \frac{1}{Q^6}$), but also contains logarithm corrections. See Appendix G from Ref. [58] for details.

For $Q^2 > 20$ GeV^2, one can represent the spectator quark model form factor F_1^* as

$$F_1^*(Q^2) \simeq -\frac{0.144}{Q^4} \log\frac{Q^2}{\Lambda^2}, \tag{33}$$

where $\Lambda^2 = 0.4982$ GeV^2.

In conclusion, our model reveals a scaling with the same power as pQCD for $Q^2 \approx 100$ GeV^2, apart from logarithm corrections. The scaling due to pQCD, if it is confirmed, will be revealed only for much larger Q^2 values than in our model.

VII. CONCLUSIONS

In this work, we applied the covariant spectator quark model to the $N(1535)$ system. We considered the simplest case where $N(1535)$ is made of states with core spin $1/2$, and we neglected the effect of the core spin $3/2$ state, as in Ref. [20]. We took also the diquark as a pointlike particle (no internal P-states). These approximations have the advantage of reducing the degrees of freedom of our model to the minimum, and to allow us to perform calculations with no adjustable parameters, since all parameters (in the quark current and wave functions) were already fixed by the study of the nucleon system [52]. Our results in this paper are then true predictions. The extension of this work to include spin $3/2$ cores (which are also part of the nucleon D-states) is in progress [66]. Once our model is calibrated for the spin $3/2$ component we will also be able of making predictions for the $N(1650)$ form factors.

Our model takes contributions for the form factors from the valence quarks alone, and neglects possible meson cloud effects (in principle dominated by η and π clouds). This approximation involving the meson cloud suppression

simplifies the construction of the $N(1535)$ wave function (as a three-quark system). Another approximation, intrinsic to the relativistic generalization that we make for the wave function, is that the $N(1535)$ state is exactly orthogonal to the nucleon state only in the case of equal masses for the two baryons $M_S = M$. However, as the orthogonal condition can be written in powers of $(M_S - M)$, one can show that our results are accurate for $Q^2 > 2.3$ GeV^2. In that region, meson cloud effects are expected to be negligible, the reason why one can make predictions for the form factors, which otherwise would contain, apart from valence quark effects, important meson cloud contributions.

For the F_1^* form factor our results are in excellent agreement with the data in the domain of applicability of our model. This is remarkable since there is no parameter adjustment. Our results for F_1^* are also close to the EBAC analysis of the quark core effects, although the EBAC results are restricted to the region $Q^2 < 2$ GeV^2.

As for the F_2^* form factor, our predictions fail completely to describe the experimental data in their sign and magnitude, which is consistent with $F_2^* \simeq 0$ for $Q^2 > 2$ GeV^2. Our results are however in good agreement with the estimations of the EBAC group of the quark core contribution to the F_2^* form factor near $Q^2 = 2$ GeV^2. These two last points suggest that our failure in describing F_2^* is caused by a large negative contribution from the meson cloud which cancels almost exactly the valence quark contribution. Although meson cloud contributions are expected to decrease with increasing Q^2, there are some exceptions to that rule, as the observed for the $\gamma N \to \Delta$ quadrupole transition form factors [59,60], where pion cloud are in fact the dominant effect. The other possible explanation for the failure of our model in the description of the F_2^*, is the internal structure of the diquark which was not considered here. But this explanation is excluded by the comparison of our results with the EBAC result, which seems to indicate that the pointlike diquark approximation is apparently good, at least for F_1^*.

A true test of the F_2^* suppression can come from the extraction of the core contributions by EBAC model for higher Q^2, planned for the near future [69], and which can confirm our results for the valence quark contributions. That test will also be useful to assert and consolidate our F_1^* results. A third independent test can be the direct comparison with lattice QCD simulations, particularly for large pion masses (say $m_\pi > 0.4$ GeV), a regime where quark-antiquark (π and η cloud) contributions are believed to be very small. Lattice QCD simulations are nowadays viable since they were performed previously for the $\gamma N \to \Delta$ and $\gamma N \to N(1440)$ reactions [71,72]. Although the comparison of phenomenological model results, at the physical pion mass point, with lattice QCD can be problematic due to the necessity of extrapolating to the physical limit; that is not a problem for the spectator quark model: it is based on a vector meson dominance parametrization of the current, and therefore can be extended successfully to the lattice conditions, as was shown for the nucleon [54] and Roper [56] reactions, for the $\gamma N \to \Delta$ transition [54,60] and also for the baryon decuplet form factors [64].

In addition to the form factors, we calculated as well the helicity amplitudes $A_{1/2}$ and $S_{1/2}$. As in our calculations the violation of the orthogonality condition between the initial and final states, gives $F_1^*(0) \propto \mathcal{I}_0(0) \neq 0$, implying that the amplitude $S_{1/2}$ diverges for $Q^2 \to 0$ and the results for F_2^* differ from the data, we conclude that helicity amplitudes are not the more convenient representation to test our model, in particular, and quark models in general. Combining our results with the hypothesis that F_2^* is negligible, because of the actual cancellation of valence quark contributions and meson cloud contributions, which is suggested by the successful comparison of the our results and the EBAC quark core contribution, we obtain an excellent description of the helicity amplitudes data, $A_{1/2}$ and $S_{1/2}$ (see dashed line in Fig. 2). As for $A_{1/2}$ the agreement is remarkable for $Q^2 > 1$ GeV^2, even before the region of validity of our model is reached. As for $S_{1/2}$, although it is singular for $Q^2 = 0$, the model describes the data for $Q^2 > 1.5$ GeV^2.

In summary, the $\gamma N \to N(1535)$ reaction is very interesting from the constituent quark model perspective. The possibility of the F_2^* form factor to vanish at intermediate Q^2 values, in contrast to what happens with all other known resonances, provides a unique challenge to theoretical models, in order to understand the role of the valence quarks, and their interplay with the meson cloud. All effort from quarks models, dynamical coupled-channel reaction models, chiral effective models and lattice QCD, are welcome in attempts that have to be harmonized and supplemented together, in order to interpret the $\gamma N \to N(1535)$ reaction data.

ACKNOWLEDGMENTS

The authors thank Hiroyuki Kamano for providing the EBAC results from Ref. [40] and Viktor Mokeev for helpful discussions. The authors also thank Franz Gross for the invitation to visit the Jefferson Lab Theory Group. G. R. was supported by the Fundação para a Ciência e a Tecnologia under the Grant No. SFRH/BPD/26886/2006. This work is also supported partially by the European Union (HadronPhysics2 project ''Study of strongly interacting matter''). The work of the two authors was also financed by the Fundação para a Ciência e a Tecnologia, under Grant No. PTDC/FIS/113940/2009, ''Hadron structure with relativistic models''.

APPENDIX A: $N(1535)$ WAVE FUNCTION

1. Nonrelativistic form

We consider now the normalization of the Ψ_{S11} wave function given by Eq. (A11) [non relativistic form]. To

represent the $N(1535)$ state in a constituent quark model framework we need to consider the momentum, spin, isospin of each quark and relate it with the $N(1535)$ proprieties. We will follow the construction based on the $SU(6) \otimes O(3)$ as in Refs. [1,3–5,15–17].

a. Jacobi momenta

We label the momentum of quark i by k_i. The center of mass momentum P is then given by $P = k_1 + k_2 + k_3$. At this point, we do not distinguish between nonrelativistic and relativistic kinematics. The Jacobi momentum are

$$k_\rho = \frac{1}{\sqrt{2}}(k_1 - k_2), \tag{A1}$$

for the relative momentum of the quark in the quark-pair (12), and

$$k_\lambda = \frac{1}{\sqrt{6}}(k_1 + k_2 - 2k_3), \tag{A2}$$

to measure the relative momentum between the diquark center of mass and the third quark. Note that k_ρ is antisymmetric in the exchange of quarks 1 and 2, and that k_λ remains unchanged (symmetric) in the same exchange.

We note that in the nonrelativistic limit and in the baryon center of mass frame ($\mathbf{k_1} + \mathbf{k_2} + \mathbf{k_3} = \mathbf{0}$) one has $\mathbf{k}_3 = -(\mathbf{k}_1 + \mathbf{k}_2)$. Therefore,

$$\mathbf{k}_\lambda = \sqrt{\frac{3}{2}}\mathbf{k}, \tag{A3}$$

where $\mathbf{k} = \mathbf{k}_1 + \mathbf{k}_2$ is the diquark three momentum.

We will use the ρ and λ labels to characterize the baryon states, as it was defined in the main text, and as it is usual practice in the literature, e.g. in Ref. [18,20].

b. Spin states

In the coupling of the spins of the 3 quarks, there are different combinations for $(s_{12}, s) = (|\mathbf{s_1} + s_2|, s)$, where s_{12} is the sum of the spins of quarks (12) and s the spin of quark (3). The possible combinations are

$$\chi^\rho = \left(0, \frac{1}{2}\right), \qquad \chi^\lambda = \left(1, \frac{1}{2}\right), \qquad \chi^S = \left(1, \frac{3}{2}\right),$$

respectively, the ρ-type (χ^ρ) and the λ-type (χ^λ) states with mixed symmetry, and the state (χ^S) which is symmetric the change of any of the three quarks.

The spin states χ^ρ and χ^λ are defined in terms of combinations of two spin states [quark-pair (12)], antisymmetric and symmetric, respectively, with the spin of the quark 3. This construction is similar to what was done for the nucleon [52,58]. One has for the spin projection $+1/2$:

$$\chi^\rho\left(+\frac{1}{2}\right) \equiv \left|\frac{1}{2}, +\frac{1}{2}\right\rangle_\rho = \frac{1}{\sqrt{2}}(\uparrow\downarrow - \downarrow\uparrow)\uparrow \tag{A4}$$

$$\chi^\lambda\left(+\frac{1}{2}\right) \equiv \left|\frac{1}{2}, +\frac{1}{2}\right\rangle_\lambda = \frac{1}{\sqrt{6}}(2\uparrow\uparrow\downarrow - \uparrow\downarrow\uparrow - \downarrow\uparrow\uparrow). \tag{A5}$$

Identical expression hold for the isospin states. For example, for the proton (isospin projection $+1/2$), we write the isospin states as

$$\begin{aligned}\phi_I^0\left(+\frac{1}{2}\right) &\equiv \frac{1}{\sqrt{2}}(ud - du)u\phi_I^1\left(+\frac{1}{2}\right) \\ &\equiv \frac{1}{\sqrt{6}}(2uud - udu - duu),\end{aligned} \tag{A6}$$

preserving the notation used in the nucleon wave function [52]. Here the antisymmetric state in the pair is identified by 0 and the symmetric state by 1.

For completeness, we represent also the state corresponding to isospin and spin projections $-1/2$:

$$\begin{aligned}\phi_I^0\left(-\frac{1}{2}\right) &\equiv \frac{1}{\sqrt{2}}(ud - du)d \\ \phi_I^1\left(-\frac{1}{2}\right) &\equiv -\frac{1}{\sqrt{6}}(2ddu - udd - dud),\end{aligned} \tag{A7}$$

$$\chi^\rho\left(-\frac{1}{2}\right) \equiv \left|\frac{1}{2}, -\frac{1}{2}\right\rangle_\rho = \frac{1}{\sqrt{2}}(\uparrow\downarrow - \downarrow\uparrow)\downarrow \tag{A8}$$

$$\chi^\lambda\left(-\frac{1}{2}\right) \equiv \left|\frac{1}{2}, -\frac{1}{2}\right\rangle_\lambda = -\frac{1}{\sqrt{6}}(2\downarrow\downarrow\uparrow - \downarrow\uparrow\downarrow - \uparrow\downarrow\downarrow). \tag{A9}$$

Later, we will write the spin states in a covariant form. In the following, we suppress the isospin projection index from $\phi_I^{0,1}$ [$+1/2$ as in the proton, and $-1/2$ as in the neutron].

c. Nucleon wave function

With the previous notation, we write the nucleon wave function for spin projection $s = \pm\frac{1}{2}$ as

$$\Psi_N = \frac{1}{\sqrt{2}}\left\{\phi_I^0\left|\frac{1}{2}, s\right\rangle_\rho + \phi_I^1\left|\frac{1}{2}, s\right\rangle_\lambda\right\}\psi_N, \tag{A10}$$

where ψ_N is a scalar wave function for the quark momentum distribution. See Ref. [52] for details about the nucleon wave function.

d. $N(1535)$ nonrelativistic wave function

The $N(1535)$ state has the same isospin structure of the nucleon. For the orbital angular momentum excitation of that state, we consider $L = 1$. We have then the form

$$\Psi_{S11} = \frac{\mathcal{N}}{\sqrt{2}}\{\phi_I^0 X_\rho - \phi_I^1 X_\lambda\}\psi_{S11}, \tag{A11}$$

with the states X_ρ and X_λ, functions of $s = \pm\frac{1}{2}$, to be defined next. The minus sign in the λ-type term is included to ensure the orthogonality with the nucleon wave function (A10). By construction, Ψ_{S11} is antisymmetric [4,20,32]. The normalization constant $\mathcal{N}$ will be determined later.

Here we take the $N(1535)$ state to be composed by states with core spin $1/2$ only. The same approximation is used in Ref. [20]. Alternative models, like the classical Karl-Isgur model [4,18], where the baryons are confined quarks with color hyperfine interaction, describe $N(1535)$ as a mixture of states with core spin $1/2$ and $3/2$ [4,18,32].

The states X_ρ and X_λ are combinations of the three-quark system mixed-symmetric states, with total spin $1/2$ (χ^ρ or χ^λ) and orbital angular momentum $L = 1$. Those states are the direct product of orbital angular momentum $L = 1$ with a spin $1/2$ state. Considering the product for the projection s, one has, for the mixed-symmetric states X_ρ:

$$X_\rho(s) = \sqrt{4\pi}\sum_m \left\langle 1m;\frac{1}{2},+\frac{1}{2}\,\middle|\,\frac{1}{2},s\right\rangle Y_{1,m}(\hat{k}_\lambda)\left|\frac{1}{2},s-m\right\rangle_\rho. \tag{A12}$$

The factor $\sqrt{4\pi}$ was introduced by convenience. Possible terms in $Y_{1m}(\hat{k}_\rho)$, associated with P states in the diquark are not considered here. This corresponds to a pointlike approximation for the diquark ($k_\rho \equiv 0$). Note that the inclusion of structure in the diquark, which demands that a dependence of the scalar wave function in k_ρ is included in general [4,18,20,32]. Here, the pointlike diquark is a first approximation.

As for the $X_\lambda(s)$ states, one has

$$X_\lambda(s) = \sqrt{4\pi}\sum_m \left\langle 1m;\frac{1}{2},+\frac{1}{2}\,\middle|\,\frac{1}{2},s\right\rangle Y_{1,m}(\hat{k}_\lambda)\left|\frac{1}{2},s-m\right\rangle_\lambda. \tag{A13}$$

Once again, we took a pointlike diquark [no terms in $Y_{1m}(\hat{k}_\rho)$].

The spherical harmonics allows us to write the angular momentum states as

$$|k_\lambda| Y_{1,+1}(\hat{k}_\lambda) = \sqrt{\frac{3}{4\pi}} k_{\lambda+} \tag{A14}$$

$$|k_\lambda| Y_{1,0}(\hat{k}_\lambda) = \sqrt{\frac{3}{4\pi}} k_{\lambda 0} \tag{A15}$$

$$|k_\lambda| Y_{1,-1}(\hat{k}_\lambda) = \sqrt{\frac{3}{4\pi}} k_{\lambda-} \tag{A16}$$

where $k_{\lambda 0} = k_{\lambda z}$, and

$$k_{\lambda\pm} = \mp\frac{1}{\sqrt{2}}(k_{\lambda x} \pm i k_{\lambda y}). \tag{A17}$$

Replacing the Clebsch-Gordan coefficients, and using the compact notation $\pm$ to represent $\pm 1/2$, one obtains:

$$\begin{aligned} X_\rho(\pm) &= \mp N\left\{k_{\lambda 0}\left|\frac{1}{2},\pm\right\rangle_\rho - \sqrt{2}k_{\lambda\pm}\left|\frac{1}{2},\mp\right\rangle_\rho\right\}. \\ X_\lambda(\pm) &= \mp N\left\{k_{\lambda 0}\left|\frac{1}{2},\pm\right\rangle_\lambda - \sqrt{2}k_{\lambda\pm}\left|\frac{1}{2},\mp\right\rangle_\lambda\right\}, \end{aligned} \tag{A18}$$

where $N = 1/|k_\lambda|$. These expressions reproduce the results from Refs. [20,32], in the pointlike diquark limit. In that case only the normalization factor differs.

e. Normalization

The normalization of Ψ_{S11} is given by Eq. (A11) [nonrelativistic form]. Details associated with parity will be discussed later in the relativistic generalization.

The wave function (A11) must be normalized in order to reproduce the $N(1535)$ charge:

$$Q_{S11} = \sum_\Lambda \int_k \Psi^\dagger_{S11}(\bar{P},k)(3j_1)\Psi_{S11}(\bar{P},k) = \frac{1}{2}(1+\tau_3). \tag{A19}$$

where Λ represents the scalar component (s) and the vectorial component (polarizations $\lambda_D = 0, \pm 1$) of the intermediate diquark, and $\bar{P} = (M_S, 0, 0, 0)$ [the momentum configuration correspondent to the rest frame].

The operator $3j_1 = \frac{1}{2} + \frac{3}{2}\tau_3$ is the quark charge operator, where τ_3 acts on the $N(1535)$ isospin states. In the following, we use the notation introduced in the paper with calculations for the nucleon [52]. We project the states into isospin components, for the case $Q^2 = 0$, according to

$$j_1 \to (\phi^0_I)^\dagger j_1 \phi^0_I = \frac{1}{6} + \frac{1}{2}\tau_3 \tag{A20}$$

$$j_3 \equiv (\phi^1_I)^\dagger j_1 \phi^1_I = \frac{1}{6} - \frac{1}{6}\tau_3. \tag{A21}$$

Then, considering (A18), one can write

$$Q_{S11} = \frac{1}{2}\mathcal{N}^2 \int_k |\psi_{S11}(\bar{P},k)|^2 [3j_1 X^\dagger_\rho X_\rho + 3j_3 X^\dagger_\lambda X_\lambda]. \tag{A22}$$

From Eqs. (A18), and working the spin algebra, for $s = \pm 1/2$, one concludes that

$$X^\dagger_\rho(s) X_\rho(s) = 1 \tag{A23}$$

$$X^\dagger_\lambda(s) X_\lambda(s) = 1. \tag{A24}$$

Then

$$\begin{aligned} Q_{S11} &= \mathcal{N}^2 \frac{3}{2}(j_1 + j_3) \int_k |\psi_{S11}(\bar{P},k)|^2 \\ &= \frac{1}{2}(1+\tau_3)\mathcal{N}^2 \int_k |\psi_{S11}(\bar{P},k)|^2, \end{aligned} \tag{A25}$$

because $3(j_1 + j_3) = (1 + \tau_3)$. Choosing

$$\int_k |\psi_{S11}(\bar{P}, k)|^2 = 1, \tag{A26}$$

and one reproduces the $N(1535)$ charge (A19), if we set $\mathcal{N} = 1$.

2. Relativistic generalization

The relativistic generalization of k_λ is the diquark three momentum in the rest frame $\tilde{k}$:

$$k_\lambda \to \tilde{k} = k - \frac{P \cdot k}{M_S^2} P, \tag{A27}$$

where P is the $N(1535)$ momentum. The factor between k_λ and k from Eq. (A3) was dropped. That factor is included into the normalization of the states. As $\tilde{k}^2 = -\mathbf{k}^2$, where $\mathbf{k}$ is the quark three momentum in the rest frame, one has

$$|k_\lambda| \to \sqrt{-\tilde{k}^2}. \tag{A28}$$

The diquark momentum components can also be defined in terms of the diquark polarization vectors:

$$\begin{aligned} k_{\lambda 0} &\to -\tilde{k} \cdot \varepsilon_P(0) \\ k_{\lambda +} &\to -\tilde{k} \cdot \varepsilon_P(+) \\ k_{\lambda -} &\to -\tilde{k} \cdot \varepsilon_P(-). \end{aligned} \tag{A29}$$

In the following, we will use ε_0 and $\varepsilon_\pm$ for, respectively, $\varepsilon_P(0)$ and $\varepsilon_P(\pm)$.

To obtain the relativistic generalization of Eq. (A11), one has to write the relativistic generalization of the spin states states $|\frac{1}{2}, s\rangle_{\rho,\lambda}$. We use the the covariant generalizations, as in the applications to the nucleon system [52,58]:

$$\left|\frac{1}{2}, s\right\rangle_\rho \to \varepsilon^s u(P, s) \tag{A30}$$

$$\left|\frac{1}{2}, s\right\rangle_\lambda \to -(\varepsilon_P^*)_\alpha U^\alpha(P, s), \tag{A31}$$

where

$$U^\alpha(P, s) = \frac{1}{\sqrt{3}} \gamma_5 \left(\gamma^\alpha - \frac{P^\alpha}{M}\right) u(P, s). \tag{A32}$$

In the previous equations, ε^s is the scalar diquark polarization $\varepsilon^s = \frac{1}{\sqrt{2}}(\uparrow\downarrow - \downarrow\uparrow)$ and ε_P the spin 1 polarization vector in the fixed-axis polarization base [52,53,58]. As ε^s is a scalar, it can replaced by 1 in the wave functions of the nucleon and $N(1535)$.

The expressions for X_ρ and X_λ from Eqs. (A18) can now be written in a relativistic form using Eqs. (A29)–(A31). The states X_ρ and X_λ are then functions of P, k (or P and $\tilde{k}$) and s, but the momentum dependence will be suppressed in our the notation. To avoid the dependence of the spin polarization in Eqs. (A18) on the normalization factor, in the relativistic generalization we replace the factor $\mp$ by -1, obtaining a unique expression for both polarizations. The final expression is then

$$X_\rho(\pm) = N[(\tilde{k} \cdot \varepsilon_0) u_S(\pm) - \sqrt{2}(\tilde{k} \cdot \varepsilon_\pm) u_S(\mp)] \tag{A33}$$

$$\begin{aligned} X_\lambda(\pm) = N[&-(\tilde{k} \cdot \varepsilon_0)(\varepsilon_P^*)_\alpha U_S^\alpha(\pm) \\ &+ \sqrt{2}(\tilde{k} \cdot \varepsilon_\pm)(\varepsilon_P^*)_\alpha U_S^\alpha(\mp)], \end{aligned} \tag{A34}$$

where we include the subindex S to label the $N(1535)$ states. In the previous equations, we have replaced the nonrelativistic constant $N = 1/|\mathbf{k}|$ by a new constant such that $|N| = 1/\sqrt{-\tilde{k}^2}$. The absolute value of N will be fixed by the comparison with the experimental data and is discussed later.

3. $N(1535)$ relativistic wave function

The final expression for the covariant $N(1535)$ wave function, with respect to spin flavor, orbital angular momentum and parity, is then

$$\Psi_{S11}(P, k) = \frac{1}{\sqrt{2}} \gamma_5 [\phi_I^0 X_\rho - \phi_I^1 X_\lambda] \psi_{S11}(P, k). \tag{A35}$$

The operator γ_5 was introduced to represent the parity of the state. The scalar wave functions were discussed in the main text (see Sect. V). Equation (A35) reproduces also the $N(1535)$ charge. With the form (A35), one has

$$\not{P} \Psi_{S11} = -M_S \Psi_{S11}. \tag{A36}$$

This relation (with the minus sign) is a consequence of the introduction of the operator γ_5 required by parity. Note that the $N(1535)$ Dirac equation, given by Eq. (A36), differs from the equations corresponding to the previous applications of the spectator quark model [52,56,58–60] (nucleon, Δ, and Roper).

In the following, we will use

$$\Psi_{S11}(P, k) = \frac{1}{\sqrt{2}} [\phi_I^0 \Phi_\rho - \phi_I^1 \Phi_\lambda] \psi_{S11}(P, k), \tag{A37}$$

where $\Phi_\rho = \gamma_5 X_\rho$ and $\Phi_\lambda = \gamma_5 X_\lambda$.

APPENDIX B: TRANSITION CURRENT

In this appendix, we calculate the electromagnetic transition current defined by Eq. (5), using the nucleon and $N(1535)$ wave functions given by Eqs. (1) and (3).

1. $N(1535)$ states

The $N(1535)$ wave function is given by Eq. (A37) with the spin states defined by (A33) and (A34). From the relations $\bar{\Phi}_\rho \equiv \Phi_\rho^\dagger \gamma^0 = -\bar{X}_\rho \gamma_5$ and $\bar{\Phi}_\lambda \equiv \Phi_\lambda^\dagger \gamma^0 = -\bar{X}_\lambda \gamma_5$, one can write

$$\bar{\Phi}_\rho(\pm) = -N[(\varepsilon_0\cdot\tilde{k})\bar{u}_S(\pm) - \sqrt{2}(\varepsilon^*_\pm\cdot\tilde{k})\bar{u}_S(\mp)]\gamma_5$$
$$\bar{\Phi}_\lambda(\pm) = N[(\varepsilon_0\cdot\tilde{k})\varepsilon_\alpha\bar{U}^\alpha_S(\pm) - \sqrt{2}(\varepsilon^*_\pm\cdot\tilde{k})\varepsilon_\alpha\bar{U}^\alpha_S(\mp)]\gamma_5. \quad \text{(B1)}$$

In the previous equations,

$$\bar{U}^{\ \alpha}_S = -\frac{1}{\sqrt{3}}\bar{u}_S\left(\gamma^\alpha - \frac{P^\alpha}{M_S}\right)\gamma_5. \quad \text{(B2)}$$

2. Properties of the states

To reduce the transition current to the standard form, one uses the properties of the nucleon and $N(1535)$ spin states U^α_S, u_S, U^α and u:

$$\begin{aligned} \not{P}_- u(P_-) &= Mu(P_-) \\ \not{P}_- U^\alpha(P_-) &= MU^\alpha(P_-) \\ \not{P}_+ u_S(P_+) &= M_S u_S(P_+) \\ \not{P}_+ U^\alpha_S(P_+) &= M_S U^\alpha_S(P_+). \end{aligned} \quad \text{(B3)}$$

Also

$$(P_+)_\alpha U^\alpha_S = 0 \quad \text{(B4)}$$

$$(P_-)_\alpha U^\alpha = 0. \quad \text{(B5)}$$

3. Integration in k

In the following, we consider the symmetries in the k integration. The evaluation of the transition current requires the determination of the integrals

$$\mathcal{I}_{\lambda'} = \int_k N(\varepsilon_{\lambda'}\cdot\tilde{k})\psi_{S11}\psi_N, \quad \text{(B6)}$$

where $\lambda' = 0, \pm$. It is easy to prove that

$$\mathcal{I}_{\pm} = 0, \quad \text{(B7)}$$

for any value of Q^2. The demonstration is trivial in the $N(1535)$ rest frame, since the product of wave functions can be written as a function of $\mathbf{k}^2$ and k_z. Then $\int_k Nk_x\psi_{S11}\psi_N = \int_k Nk_y\psi_{S11}\psi_N = 0$, because the integrand function is odd in the integration variables $k_{x,y}$. Then only $\mathcal{I}_0$ survives the k integration for a given Q^2. The case $Q^2 = 0$ will be discussed in Appendix C. The important point here, is that in the final state rest frame we have to keep in the wave function only the terms in $\tilde{k}\cdot\varepsilon_0 = -k_z$.

4. Current matrix elements

Considering the expression for the spin states and by performing the integral for the current, one obtains, for arbitrary (initial and final) spin projections:

$$\bar{\Phi}_\rho\hat{\gamma}^\mu\phi^0_S = N(\varepsilon_0\cdot\tilde{k})\bar{u}_S\hat{\gamma}^\mu\gamma_5 u \quad \text{(B8)}$$

$$\bar{\Phi}_\rho\frac{i\sigma^{\mu\nu}q_\nu}{2M}\phi^0_S = -N(\varepsilon_0\cdot\tilde{k})\bar{u}_S\frac{i\sigma^{\mu\nu}q_\nu}{2M}\gamma_5 u \quad \text{(B9)}$$

$$\bar{\Phi}_\lambda\hat{\gamma}^\mu\phi^1_S = N(\varepsilon_0\cdot\tilde{k})[\bar{U}^\alpha_S\hat{\gamma}^\mu\gamma_5 U^\beta]\Delta_{\alpha\beta} \quad \text{(B10)}$$

$$\bar{\Phi}_\lambda\frac{i\sigma^{\mu\nu}q_\nu}{2M}\phi^1_S = -N(\varepsilon_0\cdot\tilde{k})\left[\bar{U}^\alpha_S\frac{i\sigma^{\mu\nu}q_\nu}{2M}\gamma_5 U^\beta\right]\Delta_{\alpha\beta}. \quad \text{(B11)}$$

In the previous equations, $\Delta_{\alpha\beta}$ is given by Eq. (11). For the terms $i\sigma^{\mu\nu}q_\nu$ one can use the generalized Gordon identity:

$$i\sigma^{\mu\nu}q_\nu = \not{P}_+\gamma^\mu + \gamma^\mu\not{P}_- - (P_+ + P_-)^\mu. \quad \text{(B12)}$$

5. Spin algebra

The following relations holds when multiplied by $\Delta_{\alpha\beta}$:

$$\bar{U}^{\ \alpha}_S\hat{\gamma}^\mu\gamma_5 U^\beta = -\frac{1}{3}\bar{u}_S\gamma^\alpha\hat{\gamma}^\mu\gamma^\beta\gamma_5 u \quad \text{(B13)}$$

$$\bar{U}^{\ \alpha}_S\frac{i\sigma^{\mu\nu}q_\nu}{2M}\gamma_5 U^\beta = \frac{1}{3}\bar{u}_S\gamma^\alpha\frac{i\sigma^{\mu\nu}q_\nu}{2M}\gamma^\beta\gamma_5 u. \quad \text{(B14)}$$

Considering the results:

$$[\gamma^\alpha\gamma^\mu\gamma^\beta\gamma_5]\Delta_{\alpha\beta} = \gamma^\mu\gamma_5 \quad \text{(B15)}$$

$$[\gamma^\alpha\gamma^\beta\gamma_5]\Delta_{\alpha\beta} = -\gamma_5, \quad \text{(B16)}$$

one obtains

$$\bar{U}^{\ \alpha}_S\hat{\gamma}^\mu\gamma_5 U^\beta = \frac{1}{3}\bar{u}_S\hat{\gamma}^\mu\gamma_5 u \quad \text{(B17)}$$

$$\bar{U}^{\ \alpha}_S\frac{i\sigma^{\mu\nu}q_\nu}{2M}\gamma_5 U^\beta = -\frac{1}{3}\bar{u}_S\frac{i\sigma^{\mu\nu}q_\nu}{2M}\gamma_5 u. \quad \text{(B18)}$$

6. Final expressions

Using the formulas of the previous section one can write the result of the integration in k for (B8)–(B11) including also $\psi_{S11}(P_+,k)\psi_N(P_-,k)$. In the integration the relations with $(\varepsilon_0\cdot\tilde{k})$ are replaced by $\mathcal{I}_0$, defined by Eq. (14). Then

$$\int_k[\bar{\Phi}_\rho\hat{\gamma}^\mu\phi^0_S]\psi_{S11}\psi_N = \mathcal{I}_0\bar{u}_S\hat{\gamma}^\mu\gamma_5 u \quad \text{(B19)}$$

$$\int_k\left[\bar{\Phi}_\rho\frac{i\sigma^{\mu\nu}q_\nu}{2M}\phi^0_S\right]\psi_{S11}\psi_N = -\mathcal{I}_0\bar{u}_S\frac{i\sigma^{\mu\nu}q_\nu}{2M}\gamma_5 u \quad \text{(B20)}$$

$$\int_k[\bar{\Phi}_\lambda\hat{\gamma}^\mu\phi^1_S]\psi_{S11}\psi_N = -\frac{1}{3}\mathcal{I}_0\bar{u}_S\hat{\gamma}^\mu\gamma_5 u \quad \text{(B21)}$$

$$\int_k\left[\bar{\Phi}_\lambda\frac{i\sigma^{\mu\nu}q_\nu}{2M}\phi^1_S\right]\psi_{S11}\psi_N = \frac{1}{3}\mathcal{I}_0\bar{u}_S\frac{i\sigma^{\mu\nu}q_\nu}{2M}\gamma_5 u. \quad \text{(B22)}$$

Replacing the previous results in the expression for the current, we obtain

$$J^\mu = +\frac{1}{2}(3j_1 + j_3)\mathcal{I}_0\bar{u}_S\hat{\gamma}^\mu\gamma_5 u - \frac{1}{2}(3j_2 - j_4)\mathcal{I}_0\bar{u}_S\frac{i\sigma^{\mu\nu}q_\nu}{2M}\gamma_5 u. \quad \text{(B23)}$$

The previous current defines the electromagnetic transition form factors given by Eqs. (16) and (17). The sign of the normalization constant N with magnitude $|N| = 1/\sqrt{-\tilde{k}^2}$ has to be fixed by the experimental data. As the data for F_1^* is negative near $Q^2 = 0$, we choose

$$N = -\frac{1}{\sqrt{-\tilde{k}^2}}. \quad \text{(B24)}$$

APPENDIX C: OVERLAP INTEGRAL $\mathcal{I}_0$

In this appendix, we consider the integral of Eq. (14):

$$\mathcal{I}_0 = \int_k N(\varepsilon_0\cdot\tilde{k})\psi_{S11}(P_+,k)\psi_N(P_-,k). \quad \text{(C1)}$$

First, we derive an analytical expression for $\mathcal{I}_0$; next, we explore the limit cases.

1. Analytical expression

Consider the expression for the overlap integral (C1), in the $N(1535)$ rest frame

$$\mathcal{I}_0 = \int_k \frac{k_z}{|\mathbf{k}|}\psi_{S11}(P_+,k)\psi_N(P_-,k), \quad \text{(C2)}$$

where we used $\varepsilon_0\cdot\tilde{k} = -k_z$ and Eq. (B24). In the same frame one has $P_+ = (M_S,0,0,0)$, $P_- = (E,0,0,-|\mathbf{q}|)$ and $q = (\omega,0,0,|\mathbf{q}|)$, with $\omega = M_S - E$ and

$$E = \frac{M_S^2 + M^2 + Q^2}{2M_S}. \quad \text{(C3)}$$

In this case, ψ_{S11} is independent of the azimuthal angle and we can write, using $k_z = kz$:

$$\mathcal{I}_0 = \int_0^{+\infty}\frac{k^2dk}{(2\pi)^2 2E_D}\psi_{S11}(P_+\cdot k)I_z, \quad \text{(C4)}$$

where

$$I_z = \int_{-1}^{1}[z\psi_N(P_-\cdot k)]dz. \quad \text{(C5)}$$

In the previous equation we use the simplified notation for the arguments of the wave functions, since they can be represented as a scalar function of $P_\pm\cdot k$:

$$P_+\cdot k = M_S E_D, \qquad P_-\cdot k = EE_D + k_z|\mathbf{q}|. \quad \text{(C6)}$$

The separation of the function that depends on z as ψ_N from the ones depending only of k, as ψ_{S11} is possible because in the $N(1535)$ rest frame $P_+\cdot k$ is angle independent. As for ψ_N, it is represented by the simple analytical form (26). In these conditions one can evaluate I_z analytically using simple integration techniques. The result is

$$I_z = \frac{N_0}{m_D}\left(\frac{Mm_D}{2k|\mathbf{q}|}\right)^2\frac{1}{\beta_2-\beta_1}\times[\bar{\beta}_2 G_2(k,|\mathbf{q}|) - \bar{\beta}_1 G_1(k,|\mathbf{q}|)] \quad \text{(C7)}$$

where

$$\bar{\beta}_i = (\beta_i - 2) + 2\frac{EE_D}{Mm_D} \quad \text{(C8)}$$

$$G_i(k,|\mathbf{q}|) = \log\left|\frac{\bar{\beta}_i + 2\frac{k|\mathbf{q}|}{Mm_D}}{\bar{\beta}_i - 2\frac{k|\mathbf{q}|}{Mm_D}}\right|. \quad \text{(C9)}$$

To obtain the final expression, one has to perform the integration in k.

2. $\mathcal{I}_0$ in the limit $|\mathbf{q}| \to 0$

The expression obtained for I_z from Eq. (C7) does not help us to explore the limit $Q^2 \to 0$. To have a clearer idea of the Q^2 or $|\mathbf{q}|$ dependence one considers the case $|\mathbf{q}| \to 0$. In that limit one case use

$$\log\left|\frac{1+x}{1-x}\right| = 2x + \frac{2}{3}x^3 + \mathcal{O}(x^5), \quad \text{(C10)}$$

to simplify I_z. Using the previous equation with

$$x = \frac{2k}{Mm_D}\frac{|\mathbf{q}|}{\bar{\beta}_i}, \quad \text{(C11)}$$

one can conclude that

$$I_z = -\frac{4}{3}\frac{N_0}{m_D}\left(\frac{k}{Mm_D}\right)\frac{\bar{\beta}_1+\bar{\beta}_2}{\bar{\beta}_1^2\bar{\beta}_2^2}|\mathbf{q}|. \quad \text{(C12)}$$

With this relation we prove that

$$\mathcal{I}_0(Q^2) \propto |\mathbf{q}|, \quad \text{(C13)}$$

for small $|\mathbf{q}|$.

3. Two different limits

For the equal mass case ($M_S = M$), where

$$|\mathbf{q}| = \sqrt{1+\tau}Q, \quad \text{(C14)}$$

using $\tau = \frac{Q^2}{(M_S+M)^2} \equiv \frac{Q^2}{4M^2}$, one can conclude that

$$\mathcal{I}_0(Q^2) \propto Q, \quad \text{(C15)}$$

implying that $F_1^*(Q^2)$, $F_2^*(Q^2) \propto Q$ as $Q^2 \to 0$. This dependence is atypical and unexpected. Recall that the nucleon to Roper form factors vanish for $Q^2 \to 0$ with the power Q^2 (in that specific case, independently of the mass difference).

In $Q^2 = 0$ limit, and in the unequal mass case, one has

$$|\mathbf{q}| = |\mathbf{q}|_0 \equiv \frac{M_S^2 - M^2}{2M_S}. \tag{C16}$$

In this situation, one concludes that

$$\mathcal{I}_0(0) \propto \frac{M_S^2 - M^2}{2M_S}. \tag{C17}$$

This last result implies that the $S_{1/2}(Q^2)$ amplitude diverges for $M_S \neq M$. As that amplitude scales with $1/Q^2$, for $Q^2 \to 0$, if $\mathcal{I}_0(0) \neq 0$, the amplitude diverges for $Q^2 \to 0$. For the form factors F_1^* and F_2^* there is no divergence for $Q^2 \to 0$.

[1] M. M. Giannini, Rep. Prog. Phys. **54**, 453 (1991).
[2] L. Y. Glozman and D. O. Riska, Phys. Rep. **268**, 263 (1996).
[3] S. Capstick and W. Roberts, Prog. Part. Nucl. Phys. **45**, S241 (2000).
[4] N. Isgur and G. Karl, Phys. Lett. B **72**, 109 (1977); Phys. Rev. D **18**, 4187 (1978).
[5] N. Isgur and G. Karl, Phys. Rev. D **19**, 2653 (1979); **23**, 817 (1981).
[6] N. Mathur *et al.*, Phys. Lett. B **605**, 137 (2005).
[7] I. G. Aznauryan *et al.* (CLAS Collaboration), Phys. Rev. C **80**, 055203 (2009).
[8] D. Drechsel, S. S. Kamalov, and L. Tiator, Eur. Phys. J. A **34**, 69 (2007).
[9] M. M. Dalton *et al.*, Phys. Rev. C **80**, 015205 (2009).
[10] F. W. Brasse *et al.*, Z. Phys. C **22**, 33 (1984).
[11] C. S. Armstrong *et al.* (Jefferson Lab E94014 Collaboration), Phys. Rev. D **60**, 052004 (1999).
[12] R. Thompson *et al.* (CLAS Collaboration), Phys. Rev. Lett. **86**, 1702 (2001).
[13] H. Denizli *et al.* (CLAS Collaboration), Phys. Rev. C **76**, 015204 (2007).
[14] V. D. Burkert and T. S. H. Lee, Int. J. Mod. Phys. E **13**, 1035 (2004).
[15] M. Warns, H. Schroder, W. Pfeil, and H. Rollnik, Z. Phys. C **45**, 627 (1990).
[16] F. E. Close and Z. P. Li, Phys. Rev. D **42**, 2194 (1990).
[17] Z. Li and F. E. Close, Phys. Rev. D **42**, 2207 (1990).
[18] S. Capstick and B. D. Keister, Phys. Rev. D **51**, 3598 (1995).
[19] M. Aiello, M. M. Giannini, and E. Santopinto, J. Phys. G **24**, 753 (1998).
[20] I. G. Aznauryan, V. D. Burkert, and T. S. Lee, arXiv:0810.0997.
[21] Q. Zhao, B. Saghai, and Z. p. Li, J. Phys. G **28**, 1293 (2002).
[22] B. Golli and S. Sirca, Eur. Phys. J. A **47**, 61 (2011).
[23] W. Konen and H. J. Weber, Phys. Rev. D **41**, 2201 (1990).
[24] E. Pace, G. Salme, and S. Simula, Few-Body Syst. Suppl. **10**, 407 (1999); E. Pace, G. Salme, F. Cardarelli, and S. Simula, Nucl. Phys. **A666-667**, 33 (2000).
[25] J. He and Y. B. Dong, Commun. Theor. Phys. **46**, 269 (2006).
[26] C. S. An and B. S. Zou, Eur. Phys. J. A **39**, 195 (2009).
[27] V. M. Braun *et al.*, Phys. Rev. Lett. **103**, 072001 (2009).
[28] N. Kaiser, P. B. Siegel, and W. Weise, Phys. Lett. B **362**, 23 (1995).
[29] Z. Li and R. Workman, Phys. Rev. C **53**, R549 (1996).
[30] J. Nieves and E. Ruiz Arriola, Phys. Rev. D **64**, 116008 (2001).
[31] T. Inoue, E. Oset, and M. J. Vicente Vacas, Phys. Rev. C **65**, 035204 (2002).
[32] W. T. Chiang, S. N. Yang, M. Vanderhaeghen, and D. Drechsel, Nucl. Phys. **A723**, 205 (2003).
[33] T. Hyodo, D. Jido, and A. Hosaka, Phys. Rev. C **78**, 025203 (2008).
[34] D. Jido, M. Döring, and E. Oset, Phys. Rev. C **77**, 065207 (2008).
[35] M. Doring and K. Nakayama, Eur. Phys. J. A **43**, 83 (2009).
[36] E. Oset *et al.*, Prog. Theor. Phys. Suppl. **186**, 124 (2010).
[37] P. C. Bruns, M. Mai, and U. G. Meissner, Phys. Lett. B **697**, 254 (2011).
[38] G. Y. Chen, S. Kamalov, S. N. Yang, D. Drechsel, and L. Tiator, Nucl. Phys. **A723**, 447 (2003).
[39] A. Matsuyama, T. Sato, and T. S. Lee, Phys. Rep. **439**, 193 (2007).
[40] B. Julia-Diaz, H. Kamano, T. S. H. Lee, A. Matsuyama, T. Sato, and N. Suzuki, Phys. Rev. C **80**, 025207 (2009).
[41] S. Schneider, S. Krewald, and U. G. Meissner, Eur. Phys. J. A **28**, 107 (2006).
[42] M. Doring, C. Hanhart, F. Huang, S. Krewald, and U. G. Meissner, Nucl. Phys. **A829**, 170 (2009).
[43] R. Arndt, W. Briscoe, I. Strakovsky, and R. Workman, Eur. Phys. J. A **35**, 311 (2008).
[44] V. I. Mokeev, V. D. Burkert, T. S. H. Lee, L. Elouadrhiri, G. V. Fedotov, and B. S. Ishkhanov, Phys. Rev. C **80**, 045212 (2009).
[45] A. V. Anisovich, E. Klempt, V. A. Nikonov, M. A. Matveev, A. V. Sarantsev, and U. Thoma, Eur. Phys. J. A **44**, 203 (2010).
[46] M. Doring, E. Oset, and D. Strottman, Phys. Rev. C **73**, 045209 (2006).
[47] G. Penner and U. Mosel, Phys. Rev. C **66**, 055211 (2002); **66**, 055212 (2002).
[48] T. P. Vrana, S. A. Dytman, and T. S. H. Lee, Phys. Rep. **328**, 181 (2000).
[49] D. M. Manley, Int. J. Mod. Phys. A **18**, 441 (2003).
[50] J. He and Y. B. Dong, Nucl. Phys. **A725**, 201 (2003).
[51] F. Gross, Phys. Rev. **186**, 1448 (1969); F. Gross, J. W. Van Orden, and K. Holinde, Phys. Rev. C **45**, 2094 (1992).

[52] F. Gross, G. Ramalho, and M. T. Peña, Phys. Rev. C **77**, 015202 (2008).
[53] F. Gross, G. Ramalho, and M. T. Peña, Phys. Rev. C **77**, 035203 (2008).
[54] G. Ramalho and M. T. Peña, J. Phys. G **36**, 115011 (2009).
[55] F. Gross, G. Ramalho, and K. Tsushima, Phys. Lett. B **690**, 183 (2010).
[56] G. Ramalho and K. Tsushima, Phys. Rev. D **81**, 074020 (2010).
[57] G. Ramalho, F. Gross, M. T. Peña, and K. Tsushima, arXiv:1008.0371.
[58] G. Ramalho, M. T. Peña, and F. Gross, Eur. Phys. J. A **36**, 329 (2008).
[59] G. Ramalho, M. T. Peña, and F. Gross, Phys. Rev. D **78**, 114017 (2008).
[60] G. Ramalho and M. T. Peña, Phys. Rev. D **80**, 013008 (2009).
[61] G. Ramalho and M. T. Peña, J. Phys. G **36**, 085004 (2009).
[62] G. Ramalho, M. T. Peña, and F. Gross, Phys. Lett. B **678**, 355 (2009); Phys. Rev. D **81**, 113011 (2010).
[63] G. Ramalho and K. Tsushima, Phys. Rev. D **82**, 073007 (2010).
[64] G. Ramalho, K. Tsushima, and F. Gross, Phys. Rev. D **80**, 033004 (2009).
[65] G. Ramalho and M. T. Pena, Phys. Rev. D **83**, 054011 (2011).
[66] F. Gross, G. Ramalho, and M. T. Peña (work in progress).
[67] A. J. G. Hey and J. Weyers, Phys. Lett. B **48**, 69 (1974).
[68] W. N. Cottingham and I. H. Dunbar, Z. Phys. C **2**, 41 (1979).
[69] H. Kamano (private communication).
[70] C. E. Carlson and J. L. Poor, Phys. Rev. D **38**, 2758 (1988); C. E. Carlson and N. C. Mukhopadhyay, Phys. Rev. Lett. **81**, 2646 (1998).
[71] C. Alexandrou, G. Koutsou, H. Neff, J. W. Negele, W. Schroers, and A. Tsapalis, Phys. Rev. D **77**, 085012 (2008).
[72] H. W. Lin, S. D. Cohen, R. G. Edwards, and D. G. Richards, Phys. Rev. D **78**, 114508 (2008).
[73] C. Amsler *et al.* (Particle Data Group), Phys. Lett. B **667**, 1 (2008).